Springer

Available online at https://link.springer.com
http://www.jhydrod.com/
2018,30(1):23-33
https://doi.org/10.1007/s42241-018-0002-0

Five-equation and robust three-equation methods for solution verification of large eddy simulation *

Rabijit Dutta, Tao Xing
Department of Mechanical Engineering, College of Engineering, University of Idaho, Moscow, Idaho 83844-0902, USA

(Received November 14, 2017, Accepted December 23, 2017)

Abstract: This study evaluates the recently developed general framework for solution verification methods for large eddy simulation (LES) using implicitly filtered LES of periodic channel flows at friction Reynolds number of 395 on eight systematically refined grids. The seven-equation method shows that the coupling error based on Hypothesis I is much smaller as compared with the numerical and modeling errors and therefore can be neglected. The authors recommend five-equation method based on Hypothesis II, which shows a monotonic convergence behavior of the predicted numerical benchmark (S_C), and provides realistic error estimates without the need of fixing the orders of accuracy for either numerical or modeling errors. Based on the results from seven-equation and five-equation methods, less expensive three and four-equation methods for practical LES applications were derived. It was found that the new three-equation method is robust as it can be applied to any convergence types and reasonably predict the error trends. It was also observed that the numerical and modeling errors usually have opposite signs, which suggests error cancellation play an essential role in LES. When Reynolds averaged Navier-Stokes (RANS) based error estimation method is applied, it shows significant error in the prediction of S_C on coarse meshes. However, it predicts reasonable S_C when the grids resolve at least 80% of the total turbulent kinetic energy.

Key words: Large eddy simulation (LES), OpenFOAM, periodic channel flow, solution verification

Introduction

With the advent of the high-performance computing facilities, high-fidelity computational fluid dynamics (CFD) simulations using large eddy simulation (LES) are being regularly used in academic research and industrial applications. However, due to the lack of proper guidelines for verification and validation (V&V), often these simulations are either under-resolved or over-resolved. Since LES employs simpler algebraic models compared with Reynolds-averaged Navier-Stokes (RANS) based turbulence models, an under-resolved LES could be more erroneous than a RANS solution. An over-resolved LES with negligible sub-grid stress, also called quasi direct numerical simulation (DNS), provides a solution identical to a DNS solution if the same numerical algorithms are used. However, the computational cost of an LES is much greater than a DNS at the same grid due to the involvement of extra modeling terms/ equations. Therefore, quantification of numerical and modeling errors on different grid resolutions for LES is essential for significantly improving the reliability, risk assessment, and decision making of LES in scientific and engineering applications.

Various V&V methods have been established for CFD. These include grid convergence index (GCI) method and its variants[1-3], least square method[4], correction factor method[5, 6] and the factor of safety method[7, 8]. However, these V&V methods were developed for RANS based turbulence models, where the sources of errors and uncertainties can be categorized into modeling and numerical errors, and each of them can be separately evaluated. For implicitly filtered LES, local grid spacing acts as a cut-off filter, and sub-grid scale model uses the local grid spacing as the turbulent length scale parameter to model the effects of unfiltered scales on the resolved scales of motion. Therefore, the numerical and modeling errors change simultaneously when the grid size varies. As a result, they are difficult to estimate.

* **Biography:** Rabijit Dutta (1984-), Male, Ph. D.
Corresponding author: Tao Xing,
E-mail: xing@uidaho.edu

Meyers and Sagaut[9] performed a large number of LES computations in a periodic channel flow by varying the grid sizes and using the Smagorinsky model. They observed a non-monotonic grid convergence behavior and reported that along constant Nx-Ny lines, LES solutions match with fully resolved DNS even on a much coarser grid. There have been numerous attempts in quantifying the errors and uncertainties in LES using single-grid methods, viz., sub-grid activity parameter[10], modified activity parameter[11], and LES index of quality method (LES_IQ)[11]. These methods evaluated the "distance" between an LES solution and the DNS solution but did not quantify the modeling and numerical errors. These methods also involved some empirical relations that are not well tested or justified. Nevertheless, an extended version of LES_IQ based on relative resolved turbulent kinetic energy content, ($\mathrm{LES\_IQ}_k = k_{\mathrm{res}} / k_{\mathrm{tot}}$) [12] is still used[13] as a method for verification of LES solutions.

Klein[14] and Freitag and Klein[15] established the so-called systematic grid and model variation, a method for estimation of numerical and modeling errors in implicitly filtered LES. Here, the numerical and modeling errors are predicted by a systematic variation of the numerical grid and the turbulence model under the assumption that both errors can be expressed using Taylor series expansions. The main drawback of their method is the assumption of fixed scaling exponents for numerical error (P_N), equal to the theoretical order of accuracy, and modeling error (P_M) equal to 2/3 or 4/3 depending on the Reynolds number, which were not justified. Additionally, the effect of temporal discretization on the numerical error is neglected. This method was used in the LES of wind flow around high-rise buildings[13].

Xing[16] proposed the first general framework for LES V&V including a vast number methods based on two hypotheses, ranging from a sophisticated seven-equation method to a simple single grid method. In Hypothesis I, the errors and uncertainties for LES were classified into three distinct sources: numerical, modeling, and their coupling. This is the first attempt to include a coupling term for numerical and modeling errors in LES V&V. Additionally, errors and uncertainties due to grid size and time step are combined into one term, i.e., the local spatial and temporal resolution (h^* to be defined later). Hypothesis II assumes that the numerical error and modeling error can be de-coupled. For explicitly filtered LES, they can be evaluated independently by fixing the numerical variables (grid-spacing and time-step size) while systematically changing the filter width or vice versa. However, for implicitly filtered LES, the numerical variables and filter width must be refined simultaneously as to be demonstrated later. Compared to previous LES V&V, the framework does not assume the orders of accuracy for numerical and modeling errors, is applicable for both implicitly and explicitly filtered LES, and considers a systematic variation of grid spacing, time-step size, and filter width.

In the current study, the various V&V methods proposed by Xing[16] were evaluated using many datasets from LES of periodic channel flows on eight systematically refined grids and time-step sizes. Dutta and Xing[17] presented preliminary data on periodic channel flow using seven grids and showed that the numerical and modeling errors have opposite signs in six and seven-equation methods. In the next section, the methodology of LES is discussed. Then, the V&V methodology and their implementation in the current framework are briefly described followed by results, discussions, and conclusions.

1. Methodology of LES

1.1 *Governing equations*

In large eddy simulation, the Navier-Stokes equations are filtered using a low-pass filter, which leads to decomposition of all the flow variables into its filtered (or resolved) and unresolved (or sub-grid scale) components. Therefore, any variable φ, which represents either velocity or pressure can be decomposed into $\hat{\varphi}$ (resolved) and $\tilde{\varphi}$ (sub-filtered) components, $\varphi = \hat{\varphi} + \tilde{\varphi}$. The filtered component, $\hat{\varphi}$, is defined as

$$\hat{\varphi}(x,t) = \int G(x,x')\varphi(x',t)\,\mathrm{d}x' \tag{1}$$

Here x, x' and t represent the space coordinates, dummy space coordinates for each grid cell, and time coordinate, respectively. G denotes the filter or the transfer function. In the present implicitly filtered LES study, the grid size acts as a top-hat filter or box filter, which is defined as:

$$G(x,x') = \frac{1}{\Delta^3} \quad \text{for} \quad |x - x'| \le \frac{1}{2}\Delta \tag{2a}$$

$$G(x,x') = 0 \quad \text{for} \quad |x - x'| > \frac{1}{2}\Delta \tag{2b}$$

where Δ represents the size of the filter.

1.2 *Filtered Navier-Stokes equations*

Applying a filter to the incompressible Navier-Stokes equations results in the following sets of equations[18]

$$\frac{\partial \hat{u}_i}{\partial x_i} = 0 \tag{3}$$

$$\frac{\partial \hat{u}_i}{\partial t} + \frac{\partial(\hat{u}_i \hat{u}_j)}{\partial x_j} = -\frac{\partial \hat{p}}{\partial x_i} + \frac{\partial}{\partial x_j}\left\{ \nu \left[\frac{\partial \hat{u}_i}{\partial x_j} + \frac{\partial \hat{u}_j}{\partial x_i} \right] \right\} - \frac{\partial \tau_{ij}^{\mathrm{SGS}}}{\partial x_j} \tag{4}$$

Here ν represents kinematic viscosity. Applying eddy viscosity hypothesis, the sub-grid stresses, τ_{ij}^{SGS} can be presented as

$$\tau_{ij}^{\mathrm{SGS}} - \frac{1}{3}\delta_{ij}\tau_{kk}^{\mathrm{SGS}} = -2\nu_{\mathrm{SGS}}\left(\hat{S}_{ij} - \frac{1}{3}\delta_{ij}\hat{S}_{kk} \right) \tag{5}$$

Here ν_{SGS} represents the sub-grid stress eddy viscosity. $\hat{S}_{ij}$ is the symmetric part of the filtered velocity gradient tensor, also known as the filtered strain rate tensor, which is defined as, $1/2(\partial u_i/\partial x_j + \partial u_j/\partial x_i) \cdot \delta_{ij}$ denotes the Kronecker delta. In this study, the one equation eddy viscosity model[19] is used to model the effects of sub-filter scales on the resolved fields. One equation sub-grid scale (SGS) model uses a modeled balance equation to simulate the behavior of SGS kinetic energy. It overcomes the deficiency of local equilibrium assumption between SGS energy production and dissipation adopted in algebraic eddy viscosity models. Non-equilibrium turbulence spectra may occur in the coarse grid LES simulations, when the cutoff filter does not lie in the inertial spectrum[20]. The authors will perform future V&V studies using standard SGS models such as Smagorinsky model[21], dynamic Smagorinsky model[22], and WALE model[23].

1.3 *Geometry, numerical scheme and parameters*

The studied configuration is the turbulent periodic channel flow at friction Reynolds number (Re_τ) of 395. $Re_\tau = u_\tau h/\nu$, where u_τ and h denote the friction velocity and channel half-height, respectively. The setup matches with reported DNS data of Kim et al.[24]. The computational domain in the present study extends $2\pi h$, πh and $2h$ in streamwise, spanwise, and wall normal directions, respectively. Figure 1(a) schematically shows the domain, and the boundary conditions employed in the present study. Figure 1(b) shows an isosurface of $Q = 0.005$ on mesh G4.

The filtered Navier-Stokes equations are solved using an open source finite volume CFD code OpenFOAM 4.1.0. In the streamwise and spanwise directions, periodic boundary conditions are employed. A pressure gradient source is added to the streamwise momentum equation to drive the flow. The convective and diffusive terms are discretized using 2nd order central difference scheme and the time integration is performed using 2nd order implicit time. Table 1 presents the details of the grids and the time step sizes. Both the time step (Δt) and the grid spacing are simultaneously refined with a ratio of $r = \sqrt{2}$. The peak Courant number is kept below or equal to 0.5 for all the simulations. A perturbation method developed by De Villiers[25] is used to initialize the turbulence fields in the coarsest grid simulation. The simulation on the coarsest grid (G8) is first run for 20 flow-through times, and then the solutions are interpolated to the other seven grids to initialize those simulations. All the simulations are run such that once the statistically steady state is reached, time averaging is performed for additional 100 flow-through times.

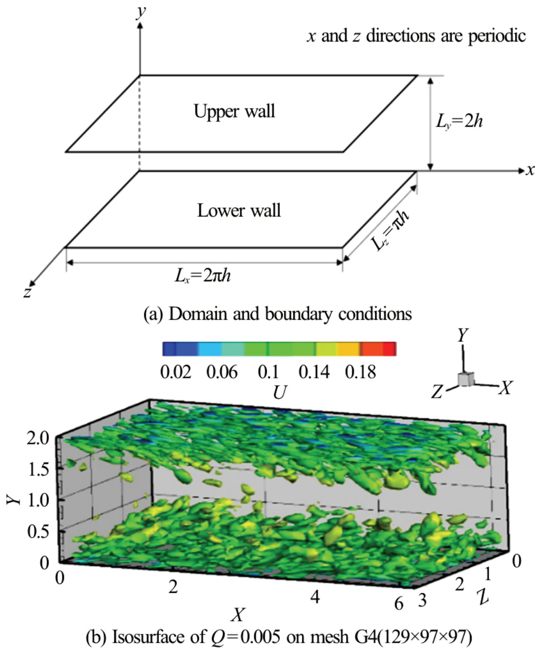

Fig. 1 (Color online) Computational geometry and vortical structures

2. Solution verification procedure

2.1 *LES error methods*

For implicitly filtered LES as adopted in this study, systematic variation of the grid-spacing and time-step sizes will simultaneously change both the numerical and modeling error terms. The local spatial and temporal resolution (h^*) is defined as

$$h^* = \sqrt{h\Delta t} \tag{6}$$

Here h and Δt represent the local grid spacing and

Table 1 Details of the grid sizes and time step sizes used in the computations; the grid spacing in x, y and z directions are presented in wall units ($\Delta x^+ = u_\tau \Delta x/\nu$, $\Delta y^+ = u_\tau \Delta y/\nu$ and $\Delta z^+ = u_\tau \Delta z/\nu$), U_b denotes the bulk velocity in the channel

Grids	N_x	N_y	N_z	Δx^+	Δy^+	Δz^+	$U_b \Delta t/h$
G1	365	272	272	6.7	0.36-7.10	4.6	0.0032
G2	257	193	193	9.5	0.45-10.00	6.5	0.0046
G3	183	137	137	13.0	0.7-14.0	9.0	0.0066
G4	129	97	97	18.0	0.9-20.0	13.0	0.0093
G5	92	68	68	24.5	1.4-28.0	18.5	0.0133
G6	65	48	48	33.0	1.8-35.0	26.0	0.0187
G7	46	34	34	54.0	2.5-55.0	36.5	0.0264
G8	33	24	24	75.0	3.5-70.0	52.0	0.0373

time step size, respectively. For implicit filtering, the local filter size (Δ) is the same as the local grid spacing (h). For a general LES simulation without any periodic directions, $\Delta(=h)$ can be calculated as

$$\Delta = \max(\Delta_x, \Delta_y, \Delta_z) \tag{7}$$

Since the flow in periodic in streamwise and spanwise directions, the solutions are averaged in these two directions. Therefore, Δ is taken as the maximum grid spacing in the y-direction. In the implicitly filtered LES as adopted in this study, systematic grid and model variation decouples the filter size and the grid size but that violates the concept of implicit filtering. Therefore, model variation is not performed. Systematic model variation can be used in the future LES V&V studies using explicit filtering. The seven-equation method based on Hypothesis I (H1-7) can be re-written as:

$$\text{G1:}\quad S_1 - S_C = \overbrace{c_N (h_*)^{p_N}}^{\delta_{SN}} + \overbrace{c_M \Delta^{p_M}}^{\delta_{SM}} + \overbrace{c_{MN} (h_* \Delta)^{p_{MN}}}^{\delta_{SMN}} \tag{8}$$

$$\text{G2:}\quad S_2 - S_C = c_N (r h_*)^{p_N} + c_M (r\Delta)^{p_M} + c_{MN} (r^2 h_* \Delta)^{p_{MN}} \tag{9}$$

$$\text{G3:}\quad S_3 - S_C = c_N (r^2 h_*)^{p_N} + c_M (r^2\Delta)^{p_M} + c_{MN} (r^4 h_* \Delta)^{p_{MN}} \tag{10}$$

$$\text{G4:}\quad S_4 - S_C = c_N (r^3 h_*)^{p_N} + c_M (r^3\Delta)^{p_M} + c_{MN} (r^6 h_* \Delta)^{p_{MN}} \tag{11}$$

$$\text{G5:}\quad S_5 - S_C = c_N (r^4 h_*)^{p_N} + c_M (r^4\Delta)^{p_M} + c_{MN} (r^8 h_* \Delta)^{p_{MN}} \tag{12}$$

$$\text{G6:}\quad S_6 - S_C = c_N (r^5 h_*)^{p_N} + c_M (r^5\Delta)^{p_M} + c_{MN} (r^{10} h_* \Delta)^{p_{MN}} \tag{13}$$

$$\text{G7:}\quad S_7 - S_C = c_N (r^6 h_*)^{p_N} + c_M (r^6\Delta)^{p_M} + c_{MN} (r^{12} h_* \Delta)^{p_{MN}} \tag{14}$$

Here δ_{SN}, δ_{SM} and δ_{SMN} denote numerical, modeling, and coupling errors, respectively. $S_i\ (i = 1-7)$ represent the solutions of the variable on the seven refined grids. For the current study, the studied variable is the u_τ. S_C represents the numerical behchmark of u_τ. P_N, P_M, P_{MN} denote the orders of accuracy for numerical, modeling and coupling error terms, respectively. C_N, C_M, C_{MN} represent the undermined constants for numerical, modeling and coupling error terms, respectively.

The set of seven nonlinear equations is then solved numerically using an optimization solver in MATLAB to obtain S_C, C_N, C_M, C_{MN}, P_N, P_M, P_{MN}. Based on this seven-equation method, simplified versions using Hypothesis I can be derived by assuming values for P_N and/or P_M, including H1-6 (fix P_N or P_M) and H1-5 (fix P_N and P_M).

The second hypothesis drops the coupling term δ_{SMN}, which eliminates two unknown variables from H1-7. As a result, H2-5 for implicitly filtered LES can be written as below:

$$\text{G1:}\quad S_1 - S_C = \overbrace{c_N (h_*)^{p_N}}^{\delta_{SN}} + \overbrace{c_M \Delta^{p_M}}^{\delta_{SM}} \tag{15}$$

$$\text{G2:}\quad S_2 - S_C = c_N (r h_*)^{p_N} + c_M (r\Delta)^{p_M} \tag{16}$$

$$\text{G3:}\quad S_3 - S_C = c_N (r^2 h_*)^{p_N} + c_M (r^2\Delta)^{p_M} \tag{17}$$

$$\text{G4:}\quad S_4 - S_C = c_N (r^3 h_*)^{p_N} + c_M (r^3\Delta)^{p_M} \tag{18}$$

$$\text{G5:}\quad S_5 - S_C = c_N (r^4 h_*)^{p_N} + c_M (r^4\Delta)^{p_M} \tag{19}$$

Similar to the seven-equation method, simplified versions using Hypothesis II can be derived by assuming values for P_N and/or P_M, including H2-4 (fixing P_N or P_M) and H2-3 (fixing P_N and P_M).

It is found that the fixing $P_M = 2$ causes the non-linear equations to be ill-posed and optimization solver does not provide any reasonable solutions. Therefore, solutions from H1-6 $(P_M = 2)$, H1-5 $(P_N = P_M = 2)$ and H2-4 $(P_M = 2)$ are not presented. As shown later, solutions from H1-7 and H2-5 suggested that the observed P_M on the finest mesh is close to 1.5, which leads to reasonable solu- tions. Therefore, H1-6 $(P_M = 1.5)$ and H2-4 $(P_M = 1.5)$ were formulated and tested. Further, a new three-equation method, H2-3 ($P_N = 1.7$ and $P_M = 1.5$) was derived and tested with equations below:

$$\text{G1:}\quad S_1 - S_C = \overbrace{c_N (h_*)^{1.7}}^{\delta_{SN}} + \overbrace{c_M \Delta^{1.5}}^{\delta_{SM}} \tag{20}$$

$$\text{G2:}\quad S_2 - S_C = c_N r^{1.7} h_*^{1.7} + c_M r^{1.5} \Delta^{1.5} \tag{21}$$

$$\text{G3:}\quad S_3 - S_C = c_N r^{3.4} h_*^{1.7} + c_M r^3 \Delta^{1.5} \tag{22}$$

Equations (20)-(22) can be solved analytically by the method of substitution:

$$C_M = \frac{r^{1.7}(S_1 - S_2) - (S_2 - S_3)}{(r^{1.7} - r^{1.5} - r^{3.2} + r^3)\Delta^{1.5}} \tag{23}$$

$$S_C = \frac{(r^{1.7} S_1 - S_2)(r^{3.2} - r^3) - (r^{1.7} S_2 - S_3)(r^{1.7} - r^{1.5})}{(r^{1.7} - 1)[(r^{3.2} - r^3) - (r^{1.7} - r^{1.5})]} \tag{24}$$

$$C_N = \frac{S_1 - S_C - C_M \Delta^{1.5}}{h_*^{1.7}} \tag{25}$$

2.2 *Solution of nonlinear equations*

Except for the three-equation method H2-3, all the LES V&V methods result in a highly non-linear system of equations. These simultaneous systems of equations were solved using the optimization toolbox, “fsolve” in MATLAB 2016. The trust-region algorithm was employed, which is based on the interior-reflective Newton method and involves the approximate solution of a large linear system using the pre-conditioned conjugate gradients method. Jacobians were analytically calculated and prescribed to the optimization solver. The solutions of a set of complex nonlinear sets of equations were found to be strongly dependant on the initial guess. S_C was initialized with a value of 0.007, which is close to the DNS solution. Other variables were provided with initial guesses in the range of 0 to 5 in a step of 0.01. The correct sets of solution were chosen based on our physical understanding of the solutions, i.e., a solution would be discarded if any one of the following conditions is met:

(1) Residual of any equation is higher than the magnitude of either numerical error or modeling error in that equation.

(2) Zero magnitudes of either numerical or modeling error.

(3) Unrealistic value of S_C.

Finally, the solution with the minimum condition number was selected.

2.3 *RANS error methods*

To evaluate the feasibility of applying existing RANS solution verification methods on LES, the errors of predicting the S_C and numerical errors itself on various grids using the former are compared with those using the various LES methods aforementioned. The typical steps for RANS solution verification start with the convergence study. If the solutions for the fine, medium and coarse grids are S_1, S_2 and S_3, respectively, solution changes ε for medium-fine and coarse-medium solutions, and the convergence ratio R is defined by

$$\varepsilon_{21} = S_2 - S_1,\quad \varepsilon_{32} = S_3 - S_2,\quad R = \frac{\varepsilon_{21}}{\varepsilon_{32}} \tag{26}$$

When monotonic convergence is achieved $(0 < R < 1)$, generalized Richardson extrapolation can be used to estimate the order-of-accuracy p_{RE}, error δ_{RE}, and numerical benchmark S_C.

$$p_{RE} = \frac{\ln\left(\dfrac{\varepsilon_{32}}{\varepsilon_{21}}\right)}{\ln(r)} \tag{27}$$

$$\delta_{RE} = \frac{\varepsilon_{21}}{r^{p_{RE}} - 1} \tag{28}$$

$$S_C = S_1 - \delta_{RE} \tag{29}$$

This approach can be applied for a grid triplet with monotonic convergence, i.e., in this study, (1, 2, 3), (2, 3, 4), (3, 4, 5), (4, 5, 6), (5, 6, 7), and (6, 7, 8) for grid refinement ratio $\sqrt{2}$. For a grid refinement ratio of 2, one can choose (1, 3, 5), (2, 4, 6), (3, 5, 7) and (4, 6, 8).

2.4 *LES index of quality index based on turbulent kinetic energy* ($\mathrm{LES\_IQ}_k$)

The fundamental idea of the $\mathrm{LES\_IQ}_k$ method is that all the eddy sizes contribute to the velocity field in a turbulent flow and LES resolves the effect of eddies which are larger than the local grid spacing (cut off filter width) and models the rest. Therefore, the resolved turbulent kinetic energy produced by LES is smaller than the turbulent kinetic energy from a wind tunnel or DNS data. Thus, $\mathrm{LES\_IQ}_k$ compares the turbulent kinetic energy resulting from the resolved scales k_{res}, with the total kinetic energy of the flow k_{tot}

$$\mathrm{LES\_IQ}_k = \frac{k_{\mathrm{res}}}{k_{\mathrm{tot}}} \tag{30}$$

Pope[18] suggested that if LES resolves 80% of the total turbulent kinetic energy, i.e., $\mathrm{LES\_IQ}_k = 0.8$, the mesh can be assumed to of sufficient resolution for LES. Celik et al.[11] proposed two ways of obtaining k_{tot}, i.e., using experimental/DNS data or by carrying out Richardson extrapolation on multiple grid simulations. Several studies reported that the second method could lead to higher turbulent kinetic energy prediction than a DNS or an experiment[13]. In this study, k_{tot} was obtained using DNS data from Kim et al.[24].

3. Results and discussion

3.1 *Mean flow and turbulence quantities*

The normalized streamwise velocity distributions from the present LES on all the eight grids are plotted in Fig. 2 and compared with the DNS data from Kim et al.[24]. In contrast to the findings from Meyers and Sagaut[9], present LES data shows a monotonic convergence with the refinement of meshes and time step sizes. Meyers and Sagaut[9] found that there is a range of coarse LES grids, which showed excellent agreement with the DNS data. However, their grids and time-steps are simultaneously varied. Figure 2 also compares the velocity fluctuations in streamwise (u_{rms}), spanwise (w_{rms}) and wall normal directions (v_{rms}) from the present LES with those of the DNS data. Present LES data show that both v_{rms} and w_{rms} values are underpredicted, which is similar to the findings of Gullbrand[26]. The errors show a monotonic convergence and decrease with the refinement of h^*. Further, as h^* becomes larger the locations of peak v_{rms} and w_{rms} are shifted away from the wall as compared DNS. u_{rms} shows a similar behavior, but with a greater offset in the location of the peak value. Peak u_{rms} value is slightly underpredicted as compared to DNS data and remains almost same on both fine and coarse grids,

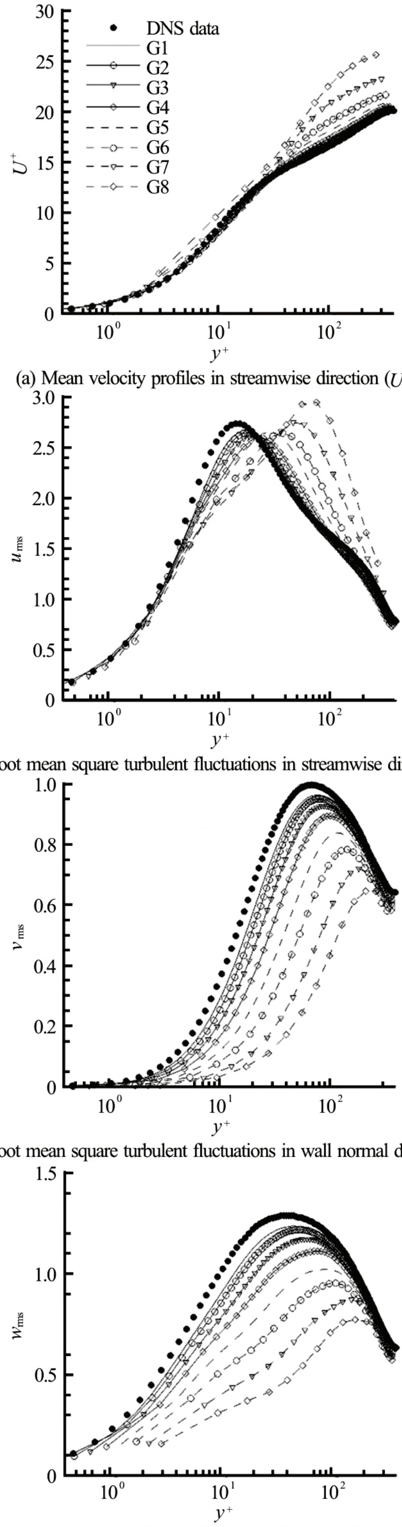

(a) Mean velocity profiles in streamwise direction (U^+)

(b) Root mean square turbulent fluctuations in streamwise direction (u_{rms})

(c) Root mean square turbulent fluctuations in wall normal direction (v_{rms})

(d) Root mean square turbulent fluctuations in spanwise direction (w_{rms})

Fig. 2 Effect of grid refinement on mean velocities and turbulent fluctuations (normalized using the friction velocity) except it marginally increased on grids G7 and G8.

Figure 3 shows the normalized k_{res} and Reynolds shear stress $(-\langle u'v'\rangle)$ from the LES solutions on various grids with a comparison to the DNS data[24]. Present LES data show that the finest two grids underpredicted the peak turbulent kinetic energy by 6%-8%DNS. The peak value of k_{res} increases monotonically with the grid refinement from G6 to G1. However, it decreases when the gridis refined from G8 to G7. Further, the peak of the k_{res} shifted farther away from the wall as the gridis coarsened. On the coarsest grid, the turbulent kinetic energy peak is observed at $y^+ \sim 75$ as compared to $y^+ \sim 15$ on the finest grid. The peak value of $(-\langle u'v'\rangle)$ shows monotonic convergence when grid is refined, with an error 3%-5 %DNS for the three finest grids. The different convergence characteristics of the normal and shear stresses need further investigation and maybe attributed to the subgrid stress model used.

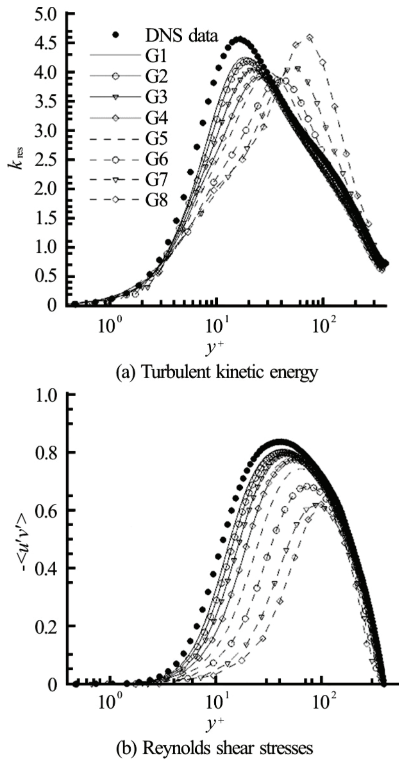

Fig. 3 Effect of grid refinement on resolved turbulent kinetic energy and Reynolds shear stresses (normalized using square of the friction velocity)

3.2 *Relation between error and LES index of quality*

Figure 4 shows the percentage error of friction velocity (u_τ) and peak Reynolds shear stress $(\langle u'v'\rangle_{\text{peak}})$ with the different grids. It also presents the LES_IQ_k on eight grids. Both errors show a monotonic convergence except on the coarsest grid for $\langle u'v'\rangle_{\text{peak}}$. LES_IQ_k shows that the three finest grids (G1-G3) resolved more than 80% of the turbulent kinetic energy.

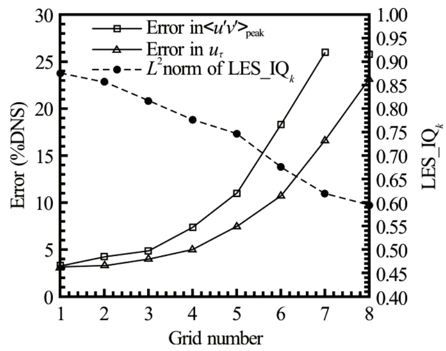

Fig. 4 Effect of grid refinement on the errors in u_τ, $\langle u'v'\rangle_{\text{peak}}$ and the corresponding LES_IQ_k $(k_{\text{res}}/k_{\text{tot}})$

3.3 *Performance of various LES V&V methods*

Table 2 presents the results for different parameters, viz., S_C and its %DNS error, P_N, P_M, P_{MN}, numerical error, modeling error, and coupling error, for various LES V&V methods using the solutions of u_τ. The H2-3 and the RANS methods were applied on solutions on all the eight grids, fixing $r = 1.414$ or 2. All the other methods were evaluated using solutions on seven grids (G1-G7). The following interpretations could be made:

(1) The stiffness of solving equations for methods

Except the three-equation method, all LES V&V methods require numerical solution of nonlinear sets of equations. The nonlinear equations are stiff and difficult to solve. As the number of equations becomes less, they are easier to solve, however, fixing $P_N = 2$, e.g., H2-4 $(P_N = 2)$, may give unreasonable solution. H2-3 is easy to implement and has analytical solution. The H1-7 method is hard to evaluate due to a large number of unknowns and solutions. It includes a wide range of meshes that resolve dramatically different flow physics. Therefore, fixing P_M and/or P_N for all the seven meshes may lead to unstable systems of equations in practical LES applications.

(2) Convergence characteristics of numerical, modeling, and coupling errors

From the limited number of reasonable solutions, H1-7 shows that the magnitude of the coupling error is at least one order of magnitude smaller than the numerical/modeling errors, which suggests that it be ignored and Hypothesis II can be adopted. H1-7 shows that the numerical and modeling errors have opposite signs, which is also observed for other methods. H2-5 indicates that the numerical error and modeling error

Table 2 Evaluation of LES error estimates

	Grids	S_C (Error %DNS)	P_N	P_M	P_{MN}	Numerical	Modeling	Coupling
H1-7	1-7	0.00765 (2.42)	1.58	1.47	1.02	-5.40×10^{-5}	1.11×10^{-5}	1.45×10^{-5}
H1-6 $(P_N = 2)$	1-6	0.00763 (2.68)	2.00	1.01	0.58	1.97×10^{-5}	6.30×10^{-4}	-6.60×10^{-4}
	2-7	0.00821 (−4.72)	2.00	1.27	0.46	-1.00×10^{-5}	3.37×10^{-4}	-8.50×10^{-4}
H1-6 $(P_M = 1.5)$	1-6	0.00764 (2.55)	1.54	1.50	0.77	-9.10×10^{-5}	9.55×10^{-5}	-4.30×10^{-5}
H2-5	1-5	0.00779 (0.64)	1.70	1.55	0	3.64×10^{-4}	-5.10×10^{-4}	0
	2-6	0.00760 (3.06)	0.78	0.72	0	-2.44×10^{-3}	2.42×10^{-3}	0
	3-7	0.00758 (3.32)	0.59	0.48	0	-2.62×10^{-3}	2.52×10^{-3}	0
H2-4 $(P_N = 2)$	1-4	0.00767 (2.17)	2.00	1.93	0	4.09×10^{-4}	-4.70×10^{-4}	0
	2-5	0.00751 (4.21)	2.00	1.95	0	-1.47×10^{-3}	1.51×10^{-5}	0
	3-6	0.00787 (−0.38)	2.00	1.89	0	1.47×10^{-3}	-1.76×10^{-5}	0
	4-7	0.00742 (5.36)	2.00	1.98	0	-3.18×10^{-3}	3.14×10^{-3}	0
H2-4 $(P_M = 1.5)$	1-4	0.00766 (2.29)	1.36	1.50	0	-4.50×10^{-4}	3.54×10^{-4}	0
	2-5	0.00779 (0.64)	1.61	1.50	0	6.38×10^{-4}	-8.22×10^{-4}	0
	3-6	0.00785 (−0.13)	1.42	1.50	0	-1.56×10^{-3}	1.26×10^{-3}	0
	4-7	0.00798 (−1.79)	1.57	1.50	0	2.98×10^{-3}	-3.49×10^{-5}	0
H2-3 ($P_M = 1.5$, $P_N = 1.7$, $r = 1.414$)	1-3	0.00756 (3.56)	1.70	1.50	0	-3.10×10^{-4}	3.42×10^{-4}	0
	2-4	0.00769 (1.98)	1.70	1.50	0	1.44×10^{-4}	-2.50×10^{-4}	0
	3-5	0.00752 (4.06)	1.70	1.50	0	-6.60×10^{-4}	6.65×10^{-4}	0
	4-6	0.00786 (−0.31)	1.70	1.50	0	7.40×10^{-4}	-1.15×10^{-3}	0
	5-7	0.00756 (3.61)	1.70	1.50	0	-4.00×10^{-4}	9.71×10^{-5}	0
	6-8	0.00817 (−4.26)	1.70	1.50	0	2.77×10^{-3}	-3.94×10^{-3}	0
H2-3 ($P_M = 1.5$, $P_N = 1.7$, $r = 2$)	1,3,5	0.00761 (2.9)	1.70	1.50	0	-8.10×10^{-5}	6.26×10^{-5}	0
	2,4,6	0.00763 (2.6)	1.70	1.50	0	-8.10×10^{-5}	2.79×10^{-5}	0
	3,5,7	0.00769 (1.98)	1.70	1.50	0	4.88×10^{-5}	-2.10×10^{-4}	0
	4,6,8	0.00776 (0.98)	1.70	1.50	0	3.01×10^{-4}	-6.20×10^{-4}	0

continuously decrease with the refinement of h^*: $(3\text{-}7) \to (2\text{-}6) \to (1\text{-}5)$. H2-4 $(P_M = 1.5)$ and H2-3 methods are easy to implement and provide reasonable estimations of numerical and modeling errors.

(3) Convergence characteristics of P_M and P_N

Solutions from H2-4 $(P_N = 2)$ shows that fixing $P_N = 2$ could force the P_M to be close to 2. This was not observed using H1-6 $(P_N = 2)$ where there is an additional coupling error term. Based on H1-7 and H2-5, P_N is close to 1.6-1.7. P_M converges towards 1.5 for the H1-7 method, which is also confirmed by the H2-5 method. H2-5 shows that, both P_M and P_N vary significantly with a variation of h^*. Assuming a $P_M = 1.5$, i.e., H2-3 ($P_M = 1.5$, $P_N = 1.7$), H2-4 $(P_M = 1.5)$ and H1-6 $(P_M = 1.5)$, provide reasonable error estimations, in contrast to fixing $P_M = 2$. This suggests that to fix P_M (or P_N) to its reasonable value such as H2-3 methods could lead to concise but accurate LES V&V methods for practical applications. Additionally, the authors believe that P_M and P_N are a function of h^* and Reynolds number.

(4) Accuracy of S_C for all methods

All the methods predicted S_C value reasonably well. The maximum error in S_C (5.4%DNS) and minimum error in S_C (0.13%DNS) are given by method H2-4 $(P_N = 2)$ for Grids 4-7 and H2-4 $(P_M = 1.5)$ for Grids 3-6, respectively. The convergence characteristics of S_C error will be discussed later with RANS.

3.4 *Comparison of LES and RANS methods*

To test the feasibility of applying RANS method for LES solutions, Fig. 5 compares the error in $S_C[(\mathrm{DNS} - S_C)/\mathrm{DNS} \times 100]$ using RANS method on multiple grid triplets ($r = 1.414$ or 2) and with the S_C errors using LES methods. H2-5 shows that error monotonically decreases when h^* is systematically refined. On the finest mesh G1, the error of S_C predicted by H2-5 is only 0.6%DNS. RANS methods and H2-3 tend to approach an S_C error around 3-3.5%DNS. For the larger grid refinement ratio r, S_C error predicted by all H2-3 methods and RANS method show monotonic convergence, whereas, for the smaller r, they show oscillatory convergence with the amplitude of the oscillation decreasing when h^* is refined. H2-4 with either fixed P_M or fixed P_N shows the error in S_C prediction around 2%. H2-4 with a fixed $P_N (= 2)$ shows an oscillatory convergence with the amplitude of the oscillation decreasing when h^* is refined, whereas, H2-4 with a fixed $P_M (=1.5)$ shows a monotonic convergence.

It is noted that RANS method on relatively coarse grids shows much larger error than H2-3 (46%DNS on Grids 6, 7, 8). However, with the refinement of h^*, the difference becomes smaller until they are almost the same after G3. This suggests that one could use traditional RANS solution verification method (e.g., the factor of safety method) to estimate S_C in LES when the mesh is fine enough. In this study, G3 resolves 81.6% of k_{tot}.

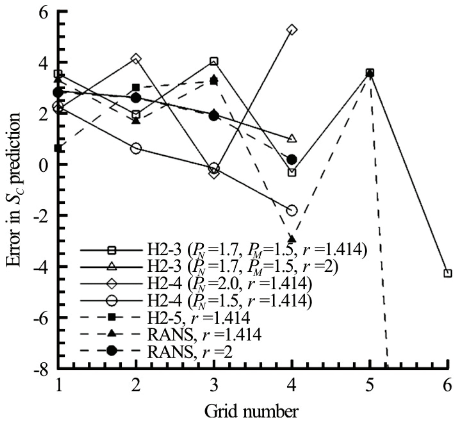

Fig. 5 Comparison of RANS and LES error estimates for S_C

3.5 *Convergence of numerical, modeling and total errors for LES V&V methods*

Figure 6 shows convergence characteristics of numerical, modeling, and total errors for H2-3, H2-4, and H2-5 with the refinement of h^*. Both H2-4 and H2-5 show that the modeling and numerical errors have opposite signs. H2-5 shows a monotonic convergence in terms of the individual error components and H2-4 shows an oscillatory convergence. For H2-3 with $r = 1.414$, numerical errors show oscillatory convergence whereas H2-3 with $r = 2$ shows monotonic convergence, which is similar to the convergence characteristics of S_C error. Modeling errors have almost the same magnitude as numerical errors and behave in the same manner except with an opposite sign. As a result of the cancellation of numerical and modeling errors, the magnitude of the total error is much smaller than either numerical or modeling error. The total error in H2-3 again shows monotonic convergence for $r = 2$ but oscillatory convergence to zero for $r = 1.414$.

3.6 *Further evaluation of the proposed three-equation method H2-3*

The three-equation method ($P_M = 1.5$ and $P_N = 1.7$) was further evaluated using contrived grid convergence studies as shown in Table 3 including monotonic convergence (MC), oscillatory convergence (OC), oscillatory divergence (OD), and monotonic divergence (MD). Fine, medium, and coarse grid solutions on each grid triplet are just copied from LES on Grids 1, 2, and 3, respectively, and one solution is varied to create the desired convergence type except for MC1. For example, the MDs are created by keeping the solutions on the coarse and medium grids to be the same as LES but the solution on the fine mesh was varied. The solutions that are the same as LES are in bold faces in Table 3. For MC1-3, RANS method was also applied (not shown). Overall the following features of the three-equation method are observed:

(1) The three-equation method is robust as it can be applied to any convergence type of LES whereas the RANS method based on Richardson Extrapolation can only be applied for monotonic convergence.

(2) For each convergence type, the three-equation method reasonably predicts the increase of the error magnitudes when the coarse grid solution is moving farther away from the other two grid solutions for MC

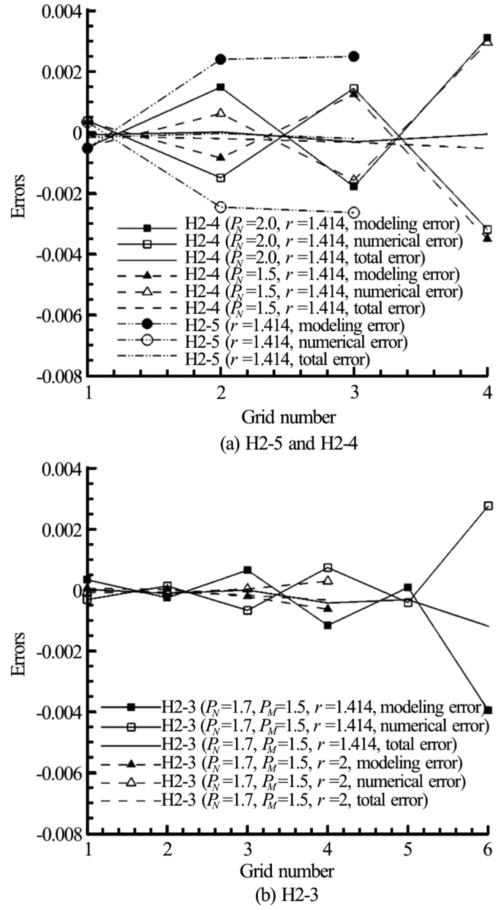

Fig. 6 Numerical, modeling, and total errors for different LES V&V methods

Table 3 Evaluation of three-equation method using contrived grid convergence studies

	Fine	Medium	Coarse	% Error in S_C	Numerical error	Modeling error	Total error
MC1	**0.0075943**	**0.0075799**	**0.0075259**	5.49	-3.081×10^{-4}	3.415×10^{-4}	3.347×10^{-5}
MC2	**0.0075943**	**0.0075799**	0.0075000	6.08	-5.758×10^{-4}	6.566×10^{-4}	8.086×10^{-3}
MC3	**0.0075943**	**0.0075799**	0.0070000	17.50	-5.737×10^{-3}	6.732×10^{-3}	9.947×10^{-4}
OC1	0.0075799	0.0075943	**0.0075259**	7.63	-9.554×10^{-4}	1.146×10^{-3}	1.902×10^{-4}
OC2	0.0075650	0.0075943	**0.0075259**	8.66	-1.215×10^{-3}	1.473×10^{-3}	2.581×10^{-4}
OC3	0.0075400	0.0075943	**0.0075259**	10.39	-1.649×10^{-3}	2.020×10^{-3}	3.716×10^{-4}
OD1	0.0075000	0.0075943	**0.0075259**	13.17	-2.343×10^{-3}	2.897×10^{-3}	5.532×10^{-4}
OD2	0.0074000	0.0075943	**0.0075259**	20.09	-4.079×10^{-3}	5.087×10^{-3}	1.007×10^{-3}
OD3	0.0073000	0.0075943	**0.0075259**	27.02	-5.816×10^{-3}	7.277×10^{-3}	1.461×10^{-3}
MD1	0.0076700	0.0075799	**0.0075259**	0.25	1.006×10^{-3}	-1.316×10^{-3}	-3.102×10^{-4}
MD2	0.0078700	0.0075799	**0.0075259**	−13.60	4.478×10^{-3}	-5.697×10^{-3}	-1.218×10^{-3}
MD3	0.0080000	0.0075799	**0.0075259**	−22.61	6.735×10^{-3}	-8.544×10^{-3}	-1.809×10^{-3}

and when the fine grid solution is moving farther away from the medium grid solution for OC, OD, and MD.

(3) Numerical and modeling errors predicted by the three-equation method have similar magnitudes and show opposite signs for all convergence types. All of them shows negative numerical errors and positive modeling errors except for MDs that show the opposite.

(4) For the three MC cases, numerical error predicted by RANS method decreases when the coarse grid solution is moving away from the other two solutions. This is due to the limitation of using Richardson Extrapolation, which leads to the use of very large factors of safety when $P > 1$ to obtain a reasonable uncertainty estimate[7]. This problem was not observed in the current three-equation method for LES V&V.

4. Conclusions and future directions

We first evaluated the general framework for solution verification of LES proposed by Xing[16] using periodic turbulent channel flow. The mean velocities and turbulence statistics are reasonably predicted on the finest grid. Further, the friction velocity and Reynolds stress predictions show monotonic convergence with the refinement of h^*, and the three finest grids in the present LES simulations resolved more than 80% of the total turbulent kinetic energy. Main findings are summarized as below:

(1) From the most sophisticated method H1-7 based on Hypothesis I, i.e., the one without assuming any values for the seven unknowns, the coupling error is at least one order of magnitude smaller than the numerical/modeling errors, which suggests that Hypothesis II is more feasible to apply as it requires much lower computational costs. The seven-equation method and the simplified six and five equations based on Hypothesis I include non-linear equations that are difficult to solve. Therefore, all the methods based on Hypothesis I are not recommended.

(2) Based on Hypothesis II, H2-5 method shows a monotonic convergence in predicting S_C, has less stiffness in the equations, and provides reasonable error estimates without assuming P_N and P_M values. Therefore, it is highly recommended.

(3) When H2-5 is too expensive due to limited computational resource, one can apply the three-equation method H2-3 ($P_M = 1.5$ and $P_N = 1.7$).

(4) Contrived grid convergence study suggests that H2-3 method is robust and can be used for monotonic convergence, monotonic divergence, oscillatory convergence and oscillatory divergence on a grid triplet.

(5) Almost all the LES V&V methods show that the numerical and modeling errors have opposite signs, which suggests error cancellation play a key role in LES.

(6) To apply existing RANS method to evaluate S_C in LES could lead to large errors on coarse meshes. However, if the grid is fine enough to resolve more than 80% of the total turbulent kinetic energy, RANS method likely predicts reasonable numerical benchmark as well.

Future work will include replicating the current approach for different Reynolds numbers, turbulence models, and numerical schemes. It is expected that after applying the current LES approach to many other cases that have DNS, one can elucidate P_M and P_N as a function of the local spatial and temporal resolution and Reynolds number, which have potential to derive more accurate solution verification methods for LES. It should be noted that the current approach based on Hypothesis II may be called implicit de-coupling where the coupling error is ignored but both numerical and modeling errors must be changed simultaneously. An alternative approach is to use explicit de-coupling for explicitly filtered LES by fixing either h^* or filter width Δ and changing the other, which allows evaluation of the numerical and modeling errors separately.

Acknowledgement

The authors would like offer gratitude to Idaho National Laboratory (INL) for providing HPC resources for running all the simulations.

References

[1] Roache P. J. Verification and validation in computational science and engineering [M]. Albuquerque, New Mexico, USA: Hermosa Publishers, 1998.

[2] Roache P. J. Fundamentals of verification and validation [M]. Albuquerque, New Mexico, USA: Hermosa Publishers, 2009.

[3] Oberkampf W. L., Roy C. J. Verification and validation in scientific computing [M]. Cambridge, UK: Cambridge University Press, 2010.

[4] Eça L., Hoekstra M. A procedure for the estimation of the numerical uncertainty of CFD calculations based on grid refinement studies [J]. *Journal of Computational Physics*, 2014, 262: 104-130.

[5] Stern F., Wilson R. V., Coleman H. W. et al. Comprehensive approach to verification and validation of CFD simulations–Part 1: Methodology and procedures [J]. *Journal of Fluids Engineering*, 2001, 123(4): 793-802.

[6] Stern F., Wilson R., Shao J. Quantitative V&V of CFD simulations and certification of CFD codes [J]. *International Journal for Numerical Methods in Fluids*, 2006, 50(11): 1335-1355.

[7] Xing T., Stern F. Factors of safety for Richardson extrapolation [J]. *Journal of Fluids Engineering*, 2010, 132(6): 061403.

[8] Xing T., Stern F. Closure to "Discussion of 'Factors of Safety for Richardson Extrapolation'" (2011, ASME J. Fluids Eng., 133, p. 115501). *Journal of Fluids Engineering-Transactions of ASME*, 2011, 133(11): 115502.

[9] Meyers J., Sagaut P. Is plane-channel flow a friendly case for the testing of large-eddy simulation subgrid-scale models? [J]. *Physics of Fluids*, 2007, 19(4): 048105.

[10] Geurts B. J., Fröhlich J. A framework for predicting accuracy limitations in large-eddy simulation [J]. *Physics of Fluids*, 2002, 14(6): L41-L42.

[11] Celik I. B., Cehreli Z. N., Yavuz I. Index of resolution quality for large eddy simulations [J]. *Journal of Fluids Engineering*, 2005, 127(5): 949-958.

[12] Celik I., Klein M., Janicka J. Assessment measures for engineering LES applications [J]. *Journal of Fluids Engineering*, 2009, 131(3): 031102.

[13] Gousseau P., Blocken B., Van Heijst G. J. F. Quality assessment of Large-Eddy Simulation of wind flow around a high-rise building: Validation and solution verification [J]. *Computers and Fluids*, 2013, 79(Suppl. C): 120-133.

[14] Klein M. An attempt to assess the quality of large eddy simulations in the context of implicit filtering [J]. *Flow, Turbulence and Combustion*, 2005, 75(1): 131-147.

[15] Freitag M., Klein M. An improved method to assess the quality of large eddy simulations in the context of implicit filtering [J]. *Journal of Turbulence*, 2006, 7: N40.

[16] Xing T. A general framework for verification and validation of large eddy simulations [J]. *Journal of Hydrodynamics*, 2015, 27(2): 163-175.

[17] Dutta R., Xing T. Quantitative solution verification of large eddy simulation of channel flow [C]. *Proceedings of the 2nd Thermal and Fluid Engineering Conference and 4th International Workshop on Heat Transfer*, Las Vegas, USA, 2017.

[18] Pope S. B.Turbulent flows [M]. Cambridge, UK: Cambridge University Press, 2000.

[19] Yoshizawa A., Horiuti K. A statistically-derived subgrid-scale kinetic energy model for the large-eddy simulation of turbulent flows [J]. *Journal of the Physical Society of Japan*, 1985, 54(8): 2834-2839.

[20] Dejoan A., Schiestel R. LES of unsteady turbulence via a one-equation subgrid-scale transport model [J]. *International Journal of Heat and Fluid Flow*, 2002, 23(4): 398-412.

[21] Smagorinsky J. General circulation experiments with the primitive equations: I. The basic experiment [J]. *Monthly Weather Review*, 1963, 91(3): 99-164.

[22] Germano M., Piomelli U., Moin P. et al. A dynamic subgrid-scale eddy viscosity model [J]. *Physics of Fluids A: Fluid Dynamics*, 1991, 3(7): 1760-1765.

[23] Nicoud F., Ducros F. Subgrid-scale stress modelling based on the square of the velocity gradient tensor, flow [J]. *Turbulence and Combustion*, 1999, 62(3): 183-200.

[24] Kim J., Moin P., Moser R. Turbulence statistics in fully developed channel flow at low Reynolds number [J]. *Journal of Fluid Mechanics*, 1987, 177: 133-166.

[25] De Villiers E. The potential of large eddy simulation for the modelling of wall bounded flows [D]. Doctoral Thesis, London, UK: University of London, 2007.

[26] Gullbrand J. Grid-independent large-eddy simulation in turbulent channel flow using three-dimensional explicit filtering [C]. *Annual research briefs: Center for Turbulence Research*, San Francisco, USA, 2003.